Glyceraldehyde-3-phosphate Dehydrogenase (GAPDH) Is Pyruvylated during 3-Bromopyruvate Mediated Cancer Cell Death

SHANMUGASUNDARAM GANAPATHY-KANNIAPPAN[1], JEAN-FRANCOIS H. GESCHWIND[1], RANI KUNJITHAPATHAM[1], MANON BUIJS[1], JOSEPHINA A. VOSSEN[1], IRINA TCHERNYSHYOV[2], ROBERT N. COLE[3], LABIQ H. SYED[1], PRAMOD P. RAO[1], SHINICHI OTA[1] and MUSTAFA VALI[1]

[1]Russell H. Morgan Department of Radiology and Radiological Sciences, [2]Department of Medicine, and the [3]Mass Spectrometry and Proteomics Facility, Johns Hopkins University School of Medicine, Baltimore, MD 21287, U.S.A.

Abstract. *Background: The pyruvic acid analog 3-bromopyruvate (3BrPA) is an alkylating agent known to induce cancer cell death by blocking glycolysis. The anti-glycolytic effect of 3BrPA is considered to be the inactivation of glycolytic enzymes. Yet, there is a lack of experimental documentation on the direct interaction of 3BrPA with any of the suggested targets during its anticancer effect. Methods and Results: In the current study, using radiolabeled (^{14}C) 3BrPA in multiple cancer cell lines, glyceraldehyde-3-phosphate dehydrogenase (GAPDH) was identified as the primary intracellular target of 3BrPA, based on two-dimensional (2D) gel electrophoretic autoradiography, mass spectrometry and immunoprecipitation. Furthermore, in vitro enzyme kinetic studies established that 3BrPA has marked affinity to GAPDH. Finally, Annexin V staining and active caspase-3 immunoblotting demonstrated that apoptosis was induced by 3BrPA. Conclusion: GAPDH pyruvylation by 3BrPA affects its enzymatic function and is the primary intracellular target in 3BrPA mediated cancer cell death.*

Tumorigenesis is a complex, multistep process, in which cells require vast amounts of ATP to support all the molecular events necessary for their exponential growth. In the presence of oxygen, normal cells use glucose oxidation in the mitochondria to generate energy for cellular function. Conversely, tumor cells display a characteristic metabolic phenotype that, even under aerobic conditions, preferentially uses glycolysis rather than oxidative phosphorylation for ATP production (1, 2). Paradoxically, the generation of ATP through glycolysis is far less efficient than ATP production through mitochondrial oxidative phosphorylation (2 *versus* 36 ATPs per glucose) and demands a constant, high supply of glucose.

Recently, interest has increased in cytotoxic drugs that act selectively affecting glycolysis in cancer cells. Specific examples of such drugs are 3-bromopyruvate (3BrPA), dichloroacetate (DCA), iodoacetic acid (IAA) and 2-deoxyglucose. The exact molecular mechanisms accounting for the cytotoxicity of these drugs are still under investigation. DCA is thought to target cancer cells by inhibiting pyruvate dehydrogenase kinase and thereby activating the pyruvate dehydrogenase complex (3). 2-Deoxyglucose blocks glycolytic energy production by non-competitive inhibition of hexokinase II (HK II) (4-6). IAA is reported to act primarily on the enzymes glyceraldehyde-3-phosphate dehydrogenase (GAPDH), 6-phosphate dehydrogenase and 6-phosphogluconate dehydrogenase (7).

The mechanism of action of 3BrPA, a halogenated pyruvate analog, has been previously ascribed to the inhibition of the enzyme HK II (8). Since 3BrPA is an alkylating agent it raises the question of whether the cytotoxic, antitumor effect of 3BrPA involves inhibition of any other targets. In this context, 3BrPA has been reported to react with the sulfhydryl and hydroxyl groups of various enzymes such as vacuolar ATPase (9), pyruvate kinase (10), macrophage migration inhibitory factor (11), ribonuclease A (12) and glutamate dehydrogenase (13). A recent study has suggested the inhibition of GAPDH and 3-phosphoglycerate kinase activity by 3BrPA (14). However, there is a lack of experimental evidence on the specific chemical interaction

Correspondence to: Jean-Francois H. Geschwind, Russell H. Morgan Department of Radiology and Radiological Sciences, Division of Vascular and Interventional Radiology, 600 North Wolfe Street, Baltimore, MD 21287, U.S.A. Tel: +1 4109557043, Fax: +1 4109550233, e-mail: jfg@jhmi.edu

Key Words: 3-Bromopyruvate, cancer cell death, GAPDH, glycolysis, Hep3B, HepG2, SK-Hep1.

of 3BrPA with any of the suggested target enzymes during 3BrPA-mediated glycolytic inhibition. In the present study, the primary intracellular targets of 3BrPA were investigated. Chemically, the 3BrPA–protein interaction is achieved by irreversible covalent binding of the pyruvyl moiety to the target protein. In order to identify the exact primary targets pyruvylated by 3BrPA, several cancer cell lines were treated with (^{14}C)-3BrPA.

Materials and Methods

Cell culture, antibodies and chemicals. Human hepatocellular carcinoma (HCC) cell lines HepG2, Hep3B and SK-Hep1 were obtained from the American Type Culture Collection (ATCC) (Manassas, VA, USA). The Vx-2 cell line was established from the rabbit Vx-2 tumor as described previously (8). All the HCC cell lines were maintained in modified Eagle's medium (ATCC) supplemented with 10% fetal bovine serum (FBS) (Hyclone Inc., South Logan, UT, USA), sodium bicarbonate and sodium pyruvate (Gibco, Carlsbad, CA, USA). The Vx-2 cell line was maintained in RPMI medium supplemented with 10% FBS. The cells were grown at 37˚C in a humidified atmosphere with 5% CO_2. All the chemicals required for the enzyme assays including purified enzymes were purchased from Sigma Chemical Co., (St Louis, MO, USA). ^{14}C-labeled 3BrPA (15 mCi/mmol) was purchased from Perkin Elmer (Waltham, Massachusetts, USA). The antibodies for GAPDH, LDH (lactate dehydrogenase), PDH (pyruvate dehydrogenase), HK II and β-actin were procured from Santa Cruz Biotechnology, Inc., (Santa Cruz, CA, USA). Active caspase-3 antibody was purchased from Novus Biologicals (Littleton, CO, USA).

SDS-PAGE, 2D gel electrophoresis and autoradiography. Cells treated with ^{14}C-3BrPA (at 200 μM concentration for 2 h) were quenched at the end of the experiment by dithiothreitol (0.5 mM) and lysed using radioimmunoprecipitation assay (RIPA) buffer supplemented with protease and phosphatase inhibitors. In brief, the harvested cells were washed with ice-cold PBS and centrifuged at 1,000 rpm for 5 min at 4˚C. The resulting pellet was re-suspended in ice-cold RIPA buffer (with protease and phosphatase inhibitors) and incubated on ice for 15 min followed by rotator shaking for 30 min in a cold room. After confirming cellular lysis under the microscope, the lysate was centrifuged at 12,000 ×g for 15 min to collect the clear supernatant containing the cellular proteins. The total protein quantity of the cell lysates was determined using a 2D-Quant kit (GE- Healthcare, Piscataway, NJ, USA). SDS-PAGE was performed using NuPAGE Bis-Tris 4-12% gels followed by either colloidal Coomassie blue staining (15) or silver staining (Bio-Rad, Hercules, CA, USA). For 2D gel electrophoresis, the samples were cleaned-up using a 2D-Clean-up kit (GE-Healthcare) and the protein was quantified by 2D-Quant kit. Isoelectric focusing was performed using Immobiline™ dry gel strips of the linear pI (isoelectric point) range 3-10, 7 cm (GE-Healthcare). The focused gel strips were subjected to second dimensional separation using NuPAGE Bis-Tris 4-12% Zoom gels (Invitrogen, Carlsbad, CA, USA), followed by colloidal Coomassie blue or silver staining. For autoradiography, samples resolved on SDS-PAGE or 2D gels were treated with radioactive "Amplify" solution (GE-Healthcare) prior to vacuum drying and exposed to X-ray film (GE-Healthcare) to obtain the images. All the procedures involving ^{14}C-3BrPA samples were used only by authorized personnel and appropriate radioactive decontaminations, containments were followed strictly according to the Johns Hopkins Radiation Safety rules and regulations.

Immunoblotting and immunoprecipitation. Western blot analysis and immunoprecipitations were performed as per standard procedures using specific antibodies. Briefly, protein samples from different cell lines were added to 4× gel loading buffer and 10× denaturing solution (Invitrogen) in appropriate proportions and incubated at 90˚C for 10 min. The samples were subjected to SDS-PAGE electrophoresis on a 4-12% Bis-Tris gradient gel (Invitrogen). The protein profiles were electroblotted to PVDF (polyvinylidene difluoride) membranes (Millipore Inc., Billerica, MA, USA) at 4˚C overnight. The antibody incubation procedures and the blocking buffer used were as per the antibody supplier's instructions. For 2D Western blot, samples were subjected to 2D gel electrophoresis followed by electroblotting and probing for specific antibody as described above. The membranes were stored for reprobing where necessary and the immunoblots were scanned for data documentation. For the immunoprecipitation experiments, the total cell lysate from cells treated with ^{14}C-3BrPA was pre-cleared, incubated with the specific antibody overnight at 4˚C with constant rotation, followed by the immune complex pulling down with Protein G Plus agarose beads (Santa Cruz Biotechnology). The immunoprecipitates were resolved on SDS-PAGE, dried and exposed to X-ray film for autoradiography.

Mass spectrometry. Protein identification from the gel spots of interest was conducted by liquid chromatography/tandem mass spectrometry (LCMS/MS). Analysis of the peptides was performed using an LTQ ion trap MS (Thermo Fisher Scientific Co., Waltham, MA, USA) or a QSTAR/Pulsar MS (Applied Biosystems/MDX Sciex Co., Foster City, CA, USA) interfaced with a 2D nanoLC system (Eksigent Technologies Inc., Dublin, CA, USA). In brief, the gel bands or spots were excised from either the colloidal Coomassie blue-stained or silver-stained gels and proteolyzed by trypsin (Promega Co., Madison, WI, USA) as previously described (16). The peptides were fractionated by reverse-phase high performance liquid chromatography (HPLC, 75 μm × 100 mm C18 column) with a 10 μm emitter using 0-60% acetonitrile/0.5% formic acid gradient over 30 min at 300 nl/min. Peptide sequences were identified using Mascot (www.matrixscience.com) or Sequest (Thermo Fisher Scientific) software to search the National Center for Biotechnology Information (NCBI) non-redundant database with the acquired fragmentation data. Identified sequences were confirmed by manually inspecting the fragmentation spectra.

Enzyme activity assays. The enzyme activity of GAPDH was determined using a KDalert™ GAPDH assay kit (Ambion Inc., Austin, TX, USA). Both purified GAPDH and the lysates from cells treated with different concentrations of 3BrPA were subjected to the activity assay. HK II activity was assayed based on the procedure of Bergmeyer *et al*. (17) as described in the Sigma Quality Control test procedure. Both purified HK II and the lysates from cells treated with different concentrations of 3BrPA were subjected to the activity assay. Enzyme activities were recorded using a Beckman Coulter DU530 UV/VIS spectrophotometer (Fullerton, CA, USA). LDH activity was assayed using a LDH assay kit from Pointe

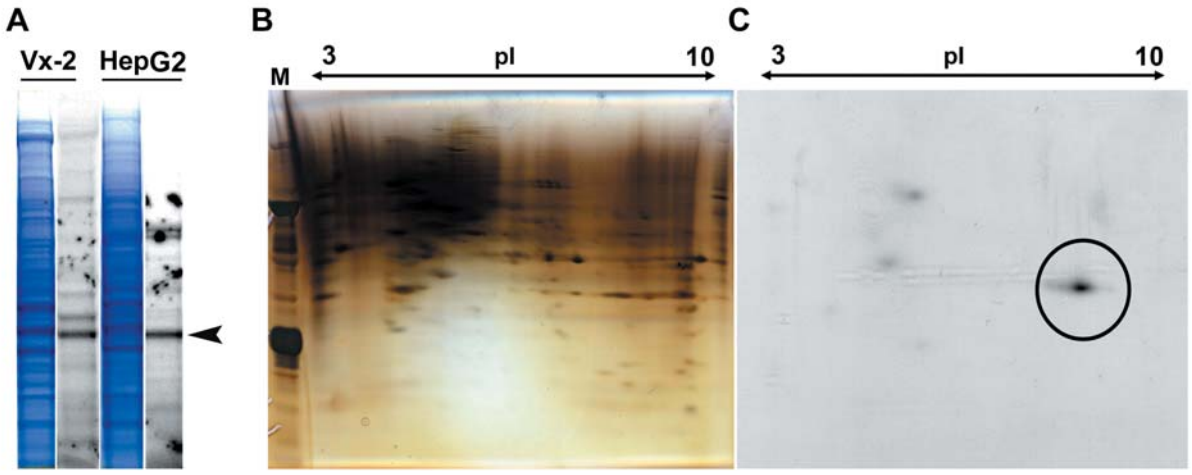

Figure 1. *Selective binding of 3BrPA to intracellular proteins. (A) Coomassie blue-stained SDS-PAGE gels and their corresponding autoradiograms are shown for HepG2 and Vx-2 cell lines treated with ^{14}C-3BrPA. Arrow head indicates the gel band excised and subjected to mass spectrometry characterization. (B) Silver-stained 2D gel of whole cell lysate from SK-Hep1 cells treated with ^{14}C-3BrPA and its corresponding autoradiogram showing ^{14}C-3BrPA incorporation. The circle indicates the intense gel spot excised and characterized by mass spectrometry.*

Scientific Co., (Canton, MI, USA). Intracellular lactate levels were quantified using a lactate assay kit from BioVision Inc., (Mountain View, CA , USA) following the manufacturer's instructions.

Determination of intracellular ATP. Cells treated with different concentrations of 3BrPA at indicated time intervals were assayed for the intracellular ATP level. Cells growing in log phase were plated in 96-well, flat-bottomed opaque plates the day before 3BrPA treatment. At the end of the treatment, ATP was quantified using a Cell Titer-Glo kit (Promega Inc.) in a Victor^3 multilabel plate reader (PerkinElmer). The cell viability or cytotoxicity was confirmed by the vital stain (Trypan blue exclusion) method.

Apoptosis assays. The apoptosis of 3BrPA treated cells was evaluated using Annexin V staining and the formation of active caspase-3. Cells treated with 3BrPA were stained with anti-Annexin V and analyzed by flow cytometry as well as fluorescent microscopy. Flow cytometry was performed using the Becton-Dikinson FACSCalibur located in the Johns Hopkins University School of Medicine, Core facility. The gating was based on unstained control cells, Annexin V – phycoerythrin (PE)-stained and 7-Amino-actinomycin D (7-AAD) stained control cells. For fluorescent microscopy, Annexin V staining was performed using an Annexin V staining Microscopy kit (BD Biosciences, San Jose, California, USA) according to the protocol recommended by the manufacturer. In brief, cells grown in chambered slides were treated with either 3BrPA or the vehicle for 2 h, washed once with ice-cold PBS followed by two washes with binding buffer, at the end of the treatment period. Then the cells were incubated with the fluorescein isothiocyanate (FITC) conjugated Annexin V fluorescent antibody for 15 min followed by a gentle wash. The cells were kept in the binding buffer and images were observed under a Zeiss Axiovert 200 Microscope (Carl Zeiss Microimaging Inc., Thornwood, NY, USA). Active caspase-3, an apoptotic marker, was identified by Western blot analysis. Lysates prepared from an equal number of cells treated with different concentrations of 3BrPA were subjected to SDS-PAGE electrophoresis and immunoblotting against active (cleaved) caspase-3.

Results

Identification of primary intracellular targets of 3BrPA. An autoradiogram of the SDS-PAGE containing protein profiles of the different cell lines (SK-Hep1, HepG2, Hep3B and Vx-2) treated with ^{14}C-3BrPA showed a strong and intense signal at the protein mass of 35-40 kDa in all four cell lines (Figures 1A, supplementary Figure S1) indicating preferential binding of ^{14}C-3BrPA. Since ^{14}C is part of the pyruvyl backbone of 3BrPA, selective binding of the pyruvyl moiety to its target(s) of the molecular mass 35-40 kDa was implied.

Even though the Coomassie-stained gel showed more than one intense band in the protein profile, the autoradiogram showed the strongest signal only at the bands within the molecular mass of 35-40 kDa. When this gel band was excised and subjected to mass spectrometry, it showed peptide sequences matching with multiple proteins (data not shown), as the one dimension gel electrophoresis is likely to have more than one polypeptide in any given protein band position. In order to identify the specific target(s) among the list of proteins identified by mass spectrometry, a 2D gel electrophoretic approach was employed. The cell lysate from SK-Hep1 cells treated with ^{14}C-3BrPA was subjected to 2D gel electrophoresis (Figure 1B) followed by autoradiography. The 2D gel showed a strong spot with intense signal at pI value ~8 and at the same molecular mass of ~37 kDa (Figure 1B). The consistency in the ^{14}C signal at ~35-40 kDa in both one dimensional as well as 2D gel electrophoresis confirmed that the 3BrPA or at least the pyruvyl group of the 3BrPA preferentially bound to one or more protein(s) of pI value ~8 and molecular size ~37 kDa.

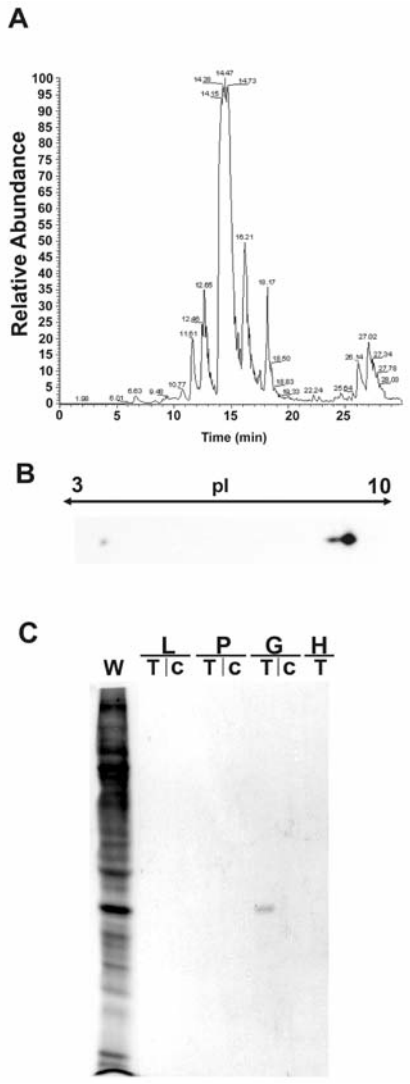

Figure 2. *GAPDH pyruvylation with 3BrPA treatment. (A) LCMS/MS chromatogram showing GAPDH as the peptide identified from autoradiogram spot of the 2D gel. (B) Immunoblot of a 2D gel showing GAPDH at the same molecular mass and pI value as the spot identified on 2D autoradiogram. (C) Autoradiogram of immunoprecipitates from the SK-Hep1 cells treated with ^{14}C-3BrPA showing the ^{14}C incorporation. Lanes indicate; W, Whole cell lysate; lanes L, P, G and H correspond to specific antibodies against the targets LDH, PDH, GAPDH and HK II, respectively. T, Target-specific antibody and C, Control IgG for the respective target.*

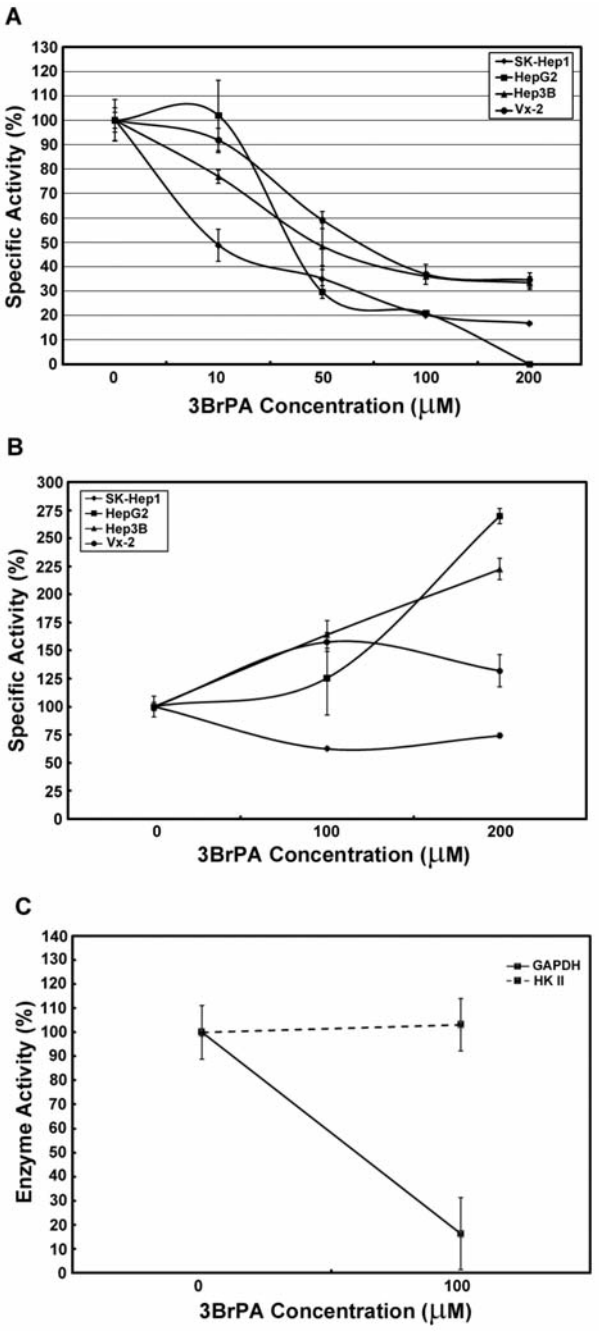

Figure 3. *Effect of pyruvylation on enzymatic function. (A) Dose-dependent decrease in the GAPDH activity in 3BrPA-treated cell lines. (B) HK II activity after 3BrPA treatment of various cell lines. (C) Activity of purified GAPDH and HK II. Equal quantities of enzymes (enzyme units) were used for these assays.*

Mass spectrometry characterization of the peptide spot (corresponding to the autoradiogram signal) from the 2D gel, gave a polypeptide sequence matching the protein, GAPDH (Figure 2A). Subsequent immunoblotting of the 2D gel containing 3BrPA treated cellular protein confirmed the spot identified by mass spectrometry (Figure 2B) as GAPDH. To further validate the finding that GAPDH is the primary intracellular target of 3BrPA, immunoprecipitation was employed for several relevant enzymes in the glycolytic pathway that could have been potential targets. Immunoprecipitation was performed for HK II, LDH, PDH and GAPDH for the lysates from cells treated with ^{14}C-3BrPA and subjected to autoradiography. The data obtained once again

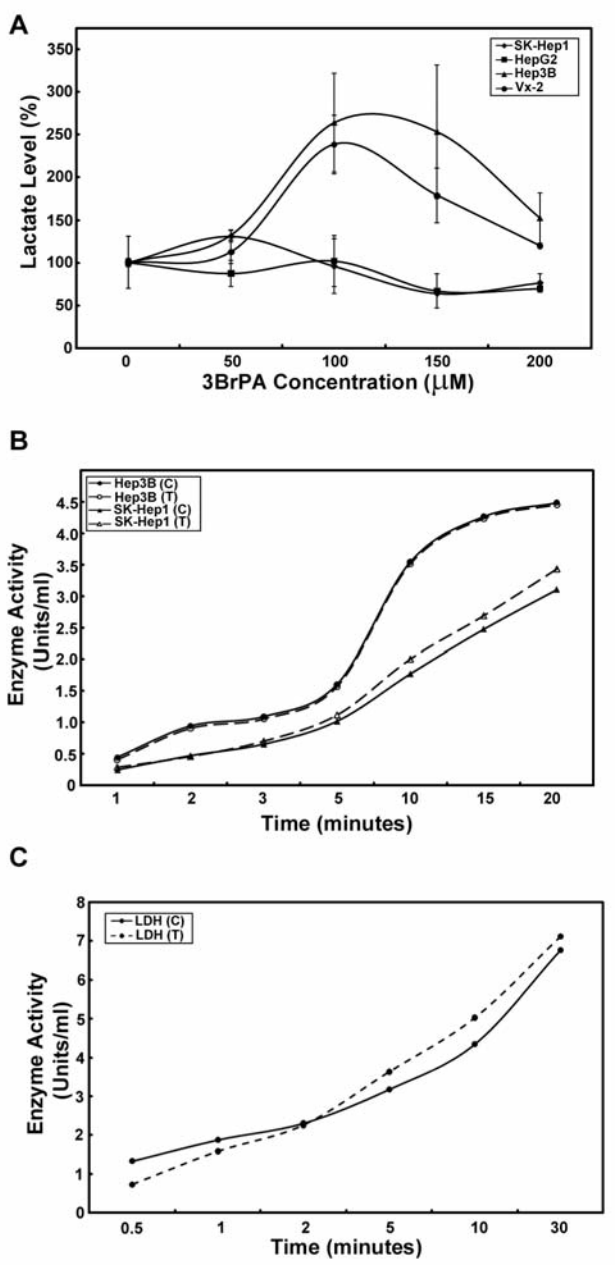

Figure 4. *Lactate levels and LDH activity in 3BrPA-treated cell lines. (A) Intracellular lactate at different concentrations of 3BrPA treatment. (B) LDH activity in SK-Hep1 and Hep3B cells in the presence or absence of 3BrPA. (C) Activity of purified LDH in the presence or absence of 3BrPA (100 μM). Results are represented as mean ± standard error (n=3). C, Control; T, treated with 3BrPA.*

demonstrated GAPDH as the primary target with incorporation of ^{14}C (Figure 2C). Together, the data from 2D gel and the immunoprecipitation autoradiograms unequivocally demonstrated that 3BrPA has a profound affinity towards GAPDH as the primary chemical target.

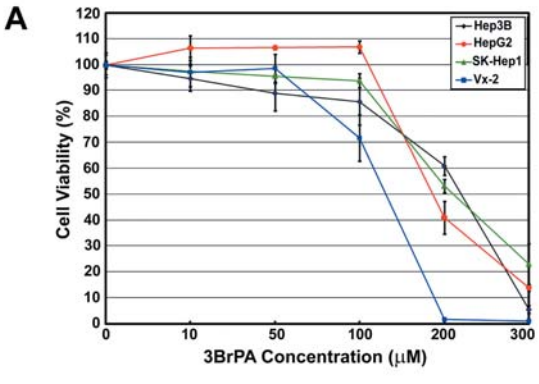

	Hep3B	HepG2	SK-Hep1	Vx-2
IC_{50} – 3BrPA (μM)	222 ± 6	187 ± 4	211 ± 3	131 ± 5

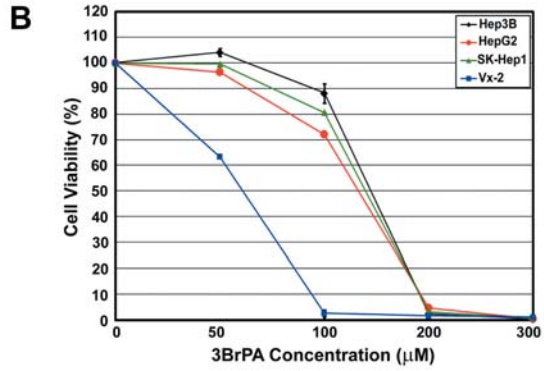

	Hep3B	HepG2	SK-Hep1	Vx-2
IC_{50} – 3BrPA (μM)	145 ±0.2	130 ± 1.3	137 ± 1.3	60 ±0.9

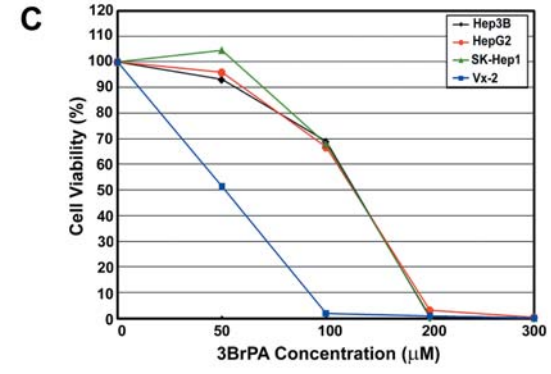

	Hep3B	HepG2	SK-Hep1	Vx-2
IC_{50} – 3BrPA (μM)	125 ± 3	125 ± 5.4	125 ± 5.8	50 ±1.8

Figure 5. *Effect of 3BrPA on the cell viability based on ATP depletion in Hep3B, HepG2, SK-Hep1 and Vx-2 cell lines. Cells were treated for (A) 3 h, (B) 24 h or (C) 48 h. Results are represented as mean ± standard error (n=3). The results were also confirmed by Trypan blue staining independently.*

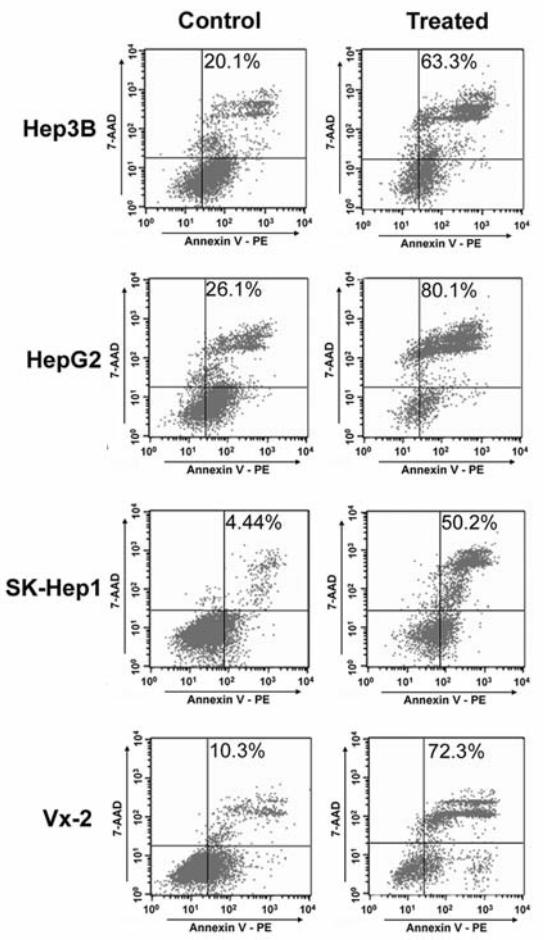

Figure 6. *Flow cytometry showing 3BrPA-induced dose-dependent apoptotic cell death. A minimum of 10^4 cells treated with 0 μM 3BrPA (Control) or 200 μM 3BrPA (Treated) for 2 h were subjected to analysis with Annexin V-PE/7-AAD staining.*

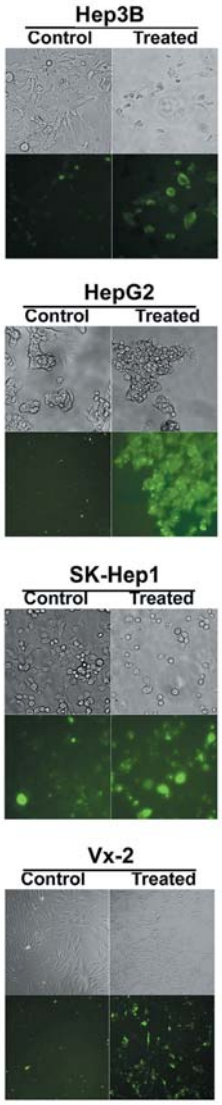

Figure 7. *Fluorescent (lower panel) and light (upper panel) micrographs showing Annexin V staining in 3BrPA (200 μM) treated cell lines and controls (vehicle alone).*

Effect of pyruvylation on enzymatic function. Based on the evidence of 3BrPA binding to GAPDH, the effect of 3BrPA interaction on the enzymatic function of GAPDH was investigated. The lysates from cells treated with different concentrations of 3BrPA showed dose-dependent attenuation of GAPDH activity in all the four cell lines (Figure 3A) supporting the notion that pyruvylation of GAPDH leads to functional impairment of the enzyme. The assays were carried out both in cell lines and in *in vitro* (purified enzyme) systems.

HK II activity remained completely unaffected by 3BrPA at cytotoxic concentration and rather showed increasing activity in at least three of the four cell lines. The only exception was the SK-Hep1 cell line where-in ~20% decreased activity was observed (Figure 3B) still retaining >75% of activity at the cytotoxic concentration (200 μM 3BrPA/2 h). As seen in Figure 3C, the GAPDH activity in an *in vitro* assay demonstrated a rapid decline (within 15 min) even at a dose of 100 μM 3BrPA (whereas HK II activity under the same conditions remained unaffected). In fact, the enzyme kinetic study of HK II showed increasing activity in a time-dependent manner even in the presence of 3BrPA (supplementary Figure S2).

The end-product of glycolysis is lactate, hence intracellular lactate levels were quantified in all the four cell lines treated with 3BrPA. The data (Figure 4A) showed an initial increase in the level of intracellular lactate followed by a decline at the lethal concentration (200 μM 3BrPA). The different cell lines showed variation in the rate of lactate production at different 3BrPA concentrations. However, the

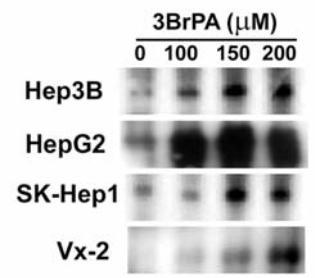

Figure 8. *Immunoblot showing caspase-3 activation by 3BrPA in different cell lines. Protein samples from equal number of cells were loaded onto each lane. The blot is a representative of duplicate experiments.*

assay of LDH activity showed that 3BrPA did not affect LDH either *in vitro* (purified LDH) or in the lysates from cells treated with 3BrPA (Figure 4B, C).

Effect of 3BrPA on ATP depletion. Treatment with 3BrPA showed a dose-dependent decrease in the level of ATP in all the four cell lines and the cytotoxicity was also linear with increasing period of treatment (Figure 5A-C). The Vx-2 cell line was more sensitive to 3BrPA than the three human HCC cell lines as inferred from the IC_{50} value of 3BrPA for each cell line at 24 h (~130 to 145 μM for HepG2, Hep3B and SK-Hep 1 cells and 60 μM for the Vx-2 cell line) and 48 h (~125 μM for HepG2, Hep3B and SK-Hep 1 cells and 50 μM for the Vx-2 cell line) of treatment (Figure 5B, C). Whereas the IC_{50} value for 3 h of treatment was comparatively higher owing to the shorter treatment period (Figure 5A). Thus increasing the duration of 3BrPA treatment resulted in decreased IC_{50} values for all the cell lines, exhibiting a typical pharmacodynamic property.

Effect of 3BrPA on apoptotic cell death. Flow cytometric analysis of all the four cell lines treated with 3BrPA using Annexin V-PE/7-AAD staining showed a dose-dependent increase in Annexin V-positive cells (Figure 6, supplementary Figure S3). Compared with control, a marked increase in apoptotic cell numbers was observed in all the cell lines after 2 h of treatment with 3BrPA. The loss of viability even in the control cells could be attributed to the cellular stress due to the downstream processing, before analysis (Figure 6). Upon normalizing the percentage of cell death in the 3BrPA treated cells with the cell death percentage of the respective control cells, all the four cell lines showed a substantial level of cell death attributed to 3BrPA treatment. Among the four cell lines Vx-2 was the most sensitive and Hep3B the least sensitive (Vx-2 >60%, HepG2>54%, SK-Hep1>45% and Hep3B>43%). This trend correlated with the IC_{50} values obtained based on the ATP viability assay for 3 h of treatment where the Vx-2 was the most sensitive followed by HepG2, SK-Hep1 and Hep3B (Figure 5A). Thus it is evident that treatment with 200 μM of 3BrPA for 3 h killed ≥50% cells among human HCC cell lines and >90% of Vx-2 cells (Figure 5A).

In order to determine whether the cytotoxic effects of 3BrPA involve cellular apoptotic pathways or not, Annexin V staining and caspase-3 activation in cells treated with 3BrPA was investigated. Figure 7 shows the photomicrographs of Annexin V staining of cells treated with 3BrPA, supporting the apoptotic form of cell death. Finally, as seen in Figure 8, immunoblotting confirmed the activation of caspase-3 during 3BrPA mediated cell death. A dose-dependent increase in active caspase-3 formation was evident in all the four cell lines treated with 3BrPA. Overall, these results support the inference that 3BrPA promoted the apoptotic form of cell death through the caspase-3 pathway in all the 3BrPA-treated cell lines.

Discussion

3BrPA has been shown to be effective as an anticancer agent in cancer cell lines and experimental animal tumor models (18-21). The present data demonstrated that covalent modification of GAPDH by the addition of the pyruvyl moiety of 3BrPA brought about the anti-glycolytic and anticancer effects. This pyruvylation of GAPDH correlated with its loss of enzymatic function. In addition, the enzymes other than GAPDH which were not pyruvylated (based on the lack of ^{14}C incorporation) remained active. The results obtained from all four cell lines demonstrated that GAPDH is the principal intracellular biochemical target of 3BrPA. Although 3BrPA is known as an alkylating agent with mixed reports implying it to be an active-site specific alkylating agent (22-26) or a non-specific alkylating agent (27-30) the present study showed for the first time that 3BrPA selectively alkylates the target, GAPDH, by pyruvylation, leading to cancer cell death.

Irrespective of the cell lines and their response/sensitivity (IC_{50}) to 3BrPA, the autoradiogram of SDS-PAGE and 2D gels showed binding of 3BrPA to a protein target between 35-40 kDa (based on the intense signal of ^{14}C incorporation). This strongly suggested that in several cell lines the mechanism of 3BrPA promoted cell death involved the pyruvylation of the same target. It remains to be elucidated how and why 3BrPA selectively targets/pyruvylates GAPDH.

It is well documented that sulfhydryl groups and cysteine amino acid residues are preferred chemical targets of 3BrPA alkylation (31-33). However, in the present study 3BrPA preferentially bound to GAPDH resulting in pyruvylation. This implies a level of specificity shown by 3BrPA in targeting intracellular proteins, however the precise mechanism or factors involved in such a selective binding are yet to be characterized. If the number of cysteine residues

determines the binding specificity, then other enzymes that have more cysteine residues (for example, HK II has four times more cysteine residues than GAPDH) should have been the preferred binding target, which was not observed in these studies. One could also argue that the abundance of GAPDH makes it a better target. However, it seems unlikely, as other abundant proteins such as β-actin or α-tubulin that are equally, if not more, abundant than GAPDH did not show any pyruvylation (based on the absence of ^{14}C incorporation). Hence it is neither the number of cysteine residues nor the intracellular abundance of the target that facilitates or favors 3BrPA binding.

The present data also showed that despite the depletion of ATP and inhibition of GAPDH, the intracellular lactate level increased substantially in all the four cell lines at lower 3BrPA concentrations. The subsequent decline in lactate level was not due to the inhibition of LDH, hence the initial increase could have been due to the production of lactate utilizing all the remaining intracellular substrates to generate ATP, while the subsequent decline at higher 3BrPA concentration indicated the complete block of GAPDH leading to reduced substrate generation for further lactate production implying complete glycolytic block. Interestingly, lactate accumulation was also reported by Pereira da Silva *et al*. (14), who showed an increase in the intracellular lactate level in 3BrPA-treated HepG2 cells which could be attributed its not being pumped out. They proposed that the intracellular accumulation of lactate was probably due to competition between lactate and 3BrPA as they both use the same transporters (mono carboxylate transporters or MCTs).

In the present report LDH activity was unaffected by 3BrPA *in vitro,* corroborating the suggestion that the intracellular accumulation of lactate was due to continuous conversion of pyruvate to lactate as long as the substrate for LDH (*i.e*. pyruvic acid) was available. However, the formation and availability of pyruvate relies on the preceding steps of glycolysis as the pyruvate is the resultant product of a series of enzymatic conversions of glucose. Since GAPDH regulates the intermediate step in the formation of pyruvate, any effect on GAPDH would hamper pyruvate formation and hence the lactate levels. The analysis of LDH activity showed it was not affected in either the Hep3B or SK-Hep1 cells at 200 μM 3BrPA, however, there was a difference in the level of intracellular lactate between these two cell lines. Interestingly, the residual GAPDH activity present in the 3BrPA (200 μM) treated cells could partially explain the difference in lactate levels, since the Hep3B cells had more residual GAPDH activity (>35%) compared to the SK-Hep1 cells (<17%). It is likely that the metabolism of downstream products of the GAPDH reaction can continue until the cell reaches a lethal state. Thus, if the GAPDH activity is low then the rate of lactate formation (one of the downstream products of glycolysis) would be less. This was supported by the intracellular lactate levels. Although HK II activity did not decrease at 200 μM 3BrPA treatment, the lactate level did not show a steady increase. Since the products of HK II have to eventually go through the GAPDH step before either being converted to lactate or entering the tricarboxylic acid cycle (TCA), it is thus the GAPDH activity that determines the rate of glycolysis and lactate formation in 3BrPA-treated cells. Based on the hypothesis suggested by Pereira da Silva *et al*. (14) that lactate accumulation is a result of a block in transport, and the present data (inhibition of GAPDH), we propose that together, the impaired transport and differential inhibition of GAPDH might contribute to the variation in intracellular lactate accumulation.

GAPDH is ubiquitous and is increasingly known for its role in multiple pathways including membrane fusion, microtubule bundling, phosphotransferase activity, nuclear RNA export, DNA replication and DNA repair (34-37), in addition to glycolysis. Thus inactivating GAPDH would affect other functions of GAPDH too. Nevertheless, several GAPDH inhibitors such as koningic acid (38, 39), methyl glyoxal (40, 41), 4-hydroxy-2-nonenal (42), phosphorylated epoxides and α-enones (43) are under investigation for their role in either antibiotic or anticancer effects. However, to our knowledge there are no other reports of any selective inhibitors targeting intracellular GAPDH, based on direct chemical interaction, particularly while promoting cell death. Since GAPDH is present in all normal tissues and 3BrPA is being evaluated as a potential cancer chemotherapeutic agent it is imperative to characterize the level of specificity shown by 3BrPA to GAPDH. Further characterization of factors that influence or control the selective targeting of GAPDH by 3BrPA would throw more light on understanding and expanding the therapeutic potential of this alkylating agent.

In conclusion, GAPDH (EC.1.2.1.12) is identified as the primary intracellular target of 3BrPA and is pyruvylated by 3BrPA which inhibits the enzymatic function of GAPDH resulting in an anti-glycolytic effect. Further, this 3BrPA-GAPDH interaction causes ATP depletion in a dose-dependent manner leading to apoptotic cell death.

Acknowledgements

This work was supported by National Institute of Health (NIH) Grant R01 CA100883-01 (Jean-Francois Geschwind), the Abdulrahman Abdulmalik Research Fund (Jean-Francois Geschwind) and the Charles Wallace Pratt Research Fund (Jean-Francois Geschwind). We thank Dr. Chi Dang, Vice-Dean for Research and Family Professor, Johns Hopkins University School of Medicine for guiding the project through intellectual input as well as logistic support. We also thank Dr. Scott Kominsky for allowing us to use the Beckman Coulter DU530 UV/VIS spectrophotometer. We thank Ms. Dawn Chen of the Proteomics Core Facility, Broadway Research Building and Mr. Richard Lee Blosser of the Flow Cytometry Facility at Ross Research Building for helping in the mass spectrometry analysis and FACS analysis respectively.

References

1 Warburg O: On the origin of cancer cells. Science *123(3191)*: 309-314, 1956.

2 Chen Z, Lu W, Garcia-Prieto C and Huang P: The Warburg effect and its cancer therapeutic implications. J Bioenerg Biomembr *39(3)*: 267-274, 2007.

3 Bonnet S, Archer SL, Allalunis-Turner J, Haromy A, Beaulieu C, Thompson R, Lee CT, Lopaschuk GD, Puttagunta L, Bonnet S, Harry G, Hashimoto K, Porter CJ, Andrade MA, Thebaud B and Michelakis ED: A mitochondria-K^+ channel axis is suppressed in cancer and its normalization promotes apoptosis and inhibits cancer growth. Cancer Cell *11*: 37-51, 2007.

4 Weindruch R, Keenan KP, Carney JM, Fernandes G, Feuers RJ, Floyd RA, Halter JB, Ramsey JJ, Richardson A, Roth GS and Spindler SR: Caloric restriction mimetics: metabolic interventions. J Gerontol A Biol Sci Med Sci *56(1)*: 20-33, 2001.

5 Maher JC, Krishan A and Lampidis TJ: Greater cell cycle inhibition and cytotoxicity induced by 2-deoxy-D-glucose in tumor cells treated under hypoxic *vs*. aerobic conditions. Cancer Chemother Pharmacol *53*: 116-122, 2004.

6 Singh D, Banerji AK, Dwarakanath BS, Tripathi RP, Gupta JP, Mathew TL, Ravindranath T and Jain V: Optimizing cancer radiotherapy with 2-deoxy-D-glucose dose escalation studies in patients with glioblastoma multiforme. Strahlenther Onkol *181*: 507-514, 2005.

7 Fahim FA, Esmat AY, Mady EA and Ibrahim EK: Antitumor activities of iodoacetate and dimethylsulphoxide against solid Ehrlich carcinoma growth in mice. Biol Res *36*: 253-262, 2003.

8 Ko YH, Pedersen PL and Geschwind JF: Glucose catabolism in the rabbit VX2 tumor model for liver cancer: characterization and targeting hexokinase. Cancer Lett *173(1)*: 83-91, 2001.

9 Dell'Antone P: Inactivation of H^+-vacuolar ATPase by the energy blocker 3-bromopyruvate, a new antitumour agent. Life Sci *79*: 2049-2055, 2006.

10 Acan NL and Ozer N: Modification of human erythrocyte pyruvate kinase by an active site-directed reagent: bromopyruvate. J Enzyme Inhib *16*: 457-464, 2001.

11 Bendrat K, Al-Abed Y, Callaway DJ, Peng T, Calandra T, Metz CN and Bucala R: Biochemical and mutational investigations of the enzymatic activity of macrophage migration inhibitory factor. Biochemistry *36*: 15356-15362, 1997.

12 Wang MH, Wang ZX and Zhao KY: Kinetics of inactivation of bovine pancreatic ribonuclease A by bromopyruvic acid. Biochem J *320(Pt 1)*: 187-192, 1996.

13 Baker JP and Rabin BR: Effects of bromopyruvate on the control and catalytic properties of glutamate dehydrogenase. Eur J Biochem *11*: 154-159, 1969.

14 Pereira da Silva AP, El-Bacha T, Kyaw N, dos Santos RS, da-Silva WS, Almeida FC, Da Poian AT and Galina A: Inhibition of energy-producing pathways of HepG2 cells by 3-bromopyruvate. Biochem J *417*: 717-726, 2009.

15 Neuhoff V, Arold N, Taube D and Ehrhardt W: Improved staining of proteins in polyacrylamide gels including isoelectric focusing gels with clear background at nanogram sensitivity using Coomassie brilliant blue G-250 and R-250. Electrophoresis *9*: 255-262, 1988.

16 Shevchenko A, Wilm M, Vorm O and Mann M: Mass spectrometric sequencing of proteins silver-stained polyacrylamide gels. Anal Chem *68*: 850-858, 1996.

17 Bergmeyer HU, Grassl M and Walter HE: Methods of enzymatic analysis. Bergmeyer HU (ed.). 3rd ed., vol. II, pp 222-223, Verlag Chemie, Deerfield Beach, FL, USA, 1983.

18 Cao X, Bloomston M, Zhang T, Frankel WL, Jia G, Wang B, Hall NC, Koch RM, Cheng H, Knopp MV and Sun D: Synergistic antipancreatic tumor effect by simultaneously targeting hypoxic cancer cells with HSP90 inhibitor and glycolysis inhibitor. Clin Cancer Res *14*: 1831-1839, 2008.

19 Xu RH, Pelicano H, Zhang H, Giles FJ, Keating MJ and Huang P: Synergistic effect of targeting mTOR by rapamycin and depleting ATP by inhibition of glycolysis in lymphoma and leukemia cells. Leukemia *19*: 2153-2158, 2005.

20 Vali M, Vossen JA, Buijs M, Engles JM, Liapi E, Ventura VP, Khwaja A, Acha-Ngwodo O, Shanmugasundaram G, Syed L, Wahl RL and Geschwind JF: Targeting of VX2 rabbit liver tumor by selective delivery of 3-bromopyruvate: a biodistribution and survival study. J Pharmacol Exp Ther *327*: 32-37, 2008.

21 Ko YH, Smith BL, Wang Y, Pomper MG, Rini DA, Torbenson MS, Hullihen J and Pedersen PL: Advanced cancers: eradication in all cases using 3-bromopyruvate therapy to deplete ATP. Biochem Biophys Res Commun *324*: 269-275, 2004.

22 Banas T, Gontero B, Drews VL, Johnson SL, Marcus F and Kemp RG: Reactivity of the thiol groups of *Escherichia coli* phosphofructo-1-kinase. Biochim Biophys Acta *957*: 178-184, 1988.

23 Honda T and Tokushige M: Active site-directed modification of tryptophanase by 3-bromopyruvate. J Biochem *97*: 851-857, 1985.

24 Kirley JW and Day RA: Irreversible inhibition of carbonic anhydrase by the carbon dioxide analog cyanogen. Biochem Biophys Res Commun *126*: 457-463, 1985.

25 Lowe PN and Perham RN: Bromopyruvate as an active-site-directed inhibitor of the pyruvate dehydrogenase multienzyme complex from *Escherichia coli*. Biochemistry *23*: 91-97, 1984.

26 Cini C, Foppoli C and De Marco C: On the product of the reaction between cysteamine and 3-bromopyruvate. Ital J Biochem *27*: 233-246, 1978.

27 Borthwick EB, Connell SJ, Tudor DW, Robins DJ, Shneier A, Abell C and Coggins JR: *Escherichia coli* dihydrodipicolinate synthase: characterization of the imine intermediate and the product of bromopyruvate treatment by electrospray mass spectrometry. Biochem J *305(Pt 2)*: 521-524, 1995.

28 Silverman PM and Eoyang L: Alkylation of acetohydroxy acid synthase I from *Escherichia coli* K-12 by 3-bromopyruvate: evidence for a single active site catalyzing acetolactate and acetohydroxybutyrate synthesis. J Bacteriol *169*: 2494-2499, 1987.

29 Yoshida H and Wood HG: Crystalline pyruvate, phosphate dikinase from *Bacteroides symbiosus*. Modification of essential histidyl residues and bromopyruvate inactivation. J Biol Chem *253*: 7650-7655, 1978.

30 Staub M and Denes G: A kinetic study on the inactivation of 3-deoxy-D-arabino-heptulosonate 7-phosphate synthase by bromopyruvate. Biochim Biophys Acta *139*: 519-521, 1967.

31 Barnett JE and Kolisis F: The reaction of *N*-acetylneuraminate lyase with chloropyruvate. Biochem J *143*: 487-490, 1974.

32 Hanau S, Bertelli M, Dallocchio F and Rippa M: Bromopyruvate for the affinity labelling of a single cysteine residue near the carboxylate binding site of lamb liver 6-phosphogluconate dehydrogenase. Biochem Mol Biol Int *37*: 785-793, 1995.

33 Salleh HM, Patel MA and Woodard RW: Essential cysteines in 3-deoxy-D-manno-octulosonic acid 8-phosphate synthase from *Escherichia coli:* analysis by chemical modification and site-directed mutagenesis. Biochemistry *35*: 8942-8947, 1996.

34 Colell A, Ricci JE, Tait S, Milasta S, Maurer U, Bouchier-Hayes L, Fitzgerald P, Guio-Carrion A, Waterhouse NJ, Li CW, Mari B, Barbry P, Newmeyer DD, Beere HM and Green DR: GAPDH and autophagy preserve survival after apoptotic cytochrome *c* release in the absence of caspase activation. Cell *129*: 983-997, 2007.

35 Du ZX, Wang HQ, Zhang HY and Gao DX: Involvement of glyceraldehyde-3-phosphate dehydrogenase in tumor necrosis factor-related apoptosis-inducing ligand-mediated death of thyroid cancer cells. Endocrinology *148*: 4352-4361, 2007.

36 Tarze A, Deniaud A, Le Bras M, Maillier E, Molle D, Larochette N, Zamzami N, Jan G, Kroemer G and Brenner C: GAPDH, a novel regulator of the pro-apoptotic mitochondrial membrane permeabilization. Oncogene *26*: 2606-2620, 2007.

37 Kim JW, Kim TE, Kim YK, Kim YW, Kim SJ, Lee JM, Kim IK and Namkoong SE: Antisense oligodeoxynucleotide of glyceraldehyde-3-phosphate dehydrogenase gene inhibits cell proliferation and induces apoptosis in human cervical carcinoma cell lines. Antisense Nucleic Acid Drug Dev *9*: 507-513, 1999.

38 Kumagai S, Narasaki R and Hasumi K: Glucose-dependent active ATP depletion by koningic acid kills high-glycolytic cells. Biochem Biophys Res Commun *365*: 362-368, 2008.

39 Nakazawa M, Uehara T and Nomura Y: Koningic acid (a potent glyceraldehyde-3-phosphate dehydrogenase inhibitor)-induced fragmentation and condensation of DNA in NG108-15 cells. J Neurochem *68*: 2493-2499, 1997.

40 Talukdar D, Ray S and Ray M: Further testing of antiviral activity of methylglyoxal urgently needed. Med Hypotheses *67*: 673-674, 2006.

41 Lee HJ, Howell SK, Sanford RJ and Beisswenger PJ: Methylglyoxal can modify GAPDH activity and structure. Ann NY Acad Sci *1043*: 135-145, 2005.

42 Ishii T, Tatsuda E, Kumazawa S, Nakayama T and Uchida K: Molecular basis of enzyme inactivation by an endogenous electrophile 4-hydroxy-2-nonenal: identification of modification sites in glyceraldehyde-3-phosphate dehydrogenase. Biochemistry *42*: 3474-3480, 2003.

43 Willson M, Lauth N, Perie J, Callens M and Opperdoes FR: Inhibition of glyceraldehyde-3-phosphate dehydrogenase by phosphorylated epoxides and alpha-enones. Biochemistry *33*: 214-220, 1994.

Received August 13, 2009
Revised November 5, 2009
Accepted November 10, 2009